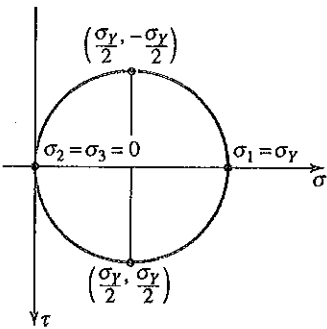


multiaxial loading, it is necessary to consider the actual mechanism of failure. That is, was failure caused by the maximum normal stress reaching a critical value? Or was it due to maximum shear stress that reached a critical value, or to strain energy or some other quantity having reached its critical value? In the tension test, the criterion for failure can be easily stated in terms of the principal (tensile) stress σ_1 , but for multiaxial stress we must consider the actual cause of the failure and say what combinations of stress would constitute failure.

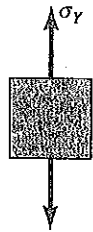
In this section we consider four theories of failure.² Two of these apply to materials that behave in a ductile manner, that is, to materials that yield before they fracture. The other two theories apply to brittle materials. For plane stress, the failure theories are expressed in terms of the principal stresses σ_1 and σ_2 . For triaxial states of stress, σ_1 , σ_2 , and σ_3 are used.

Ductile Materials. Two theories of failure for ductile materials will be discussed, the maximum-shear-stress theory and the maximum-distortion-energy theory.

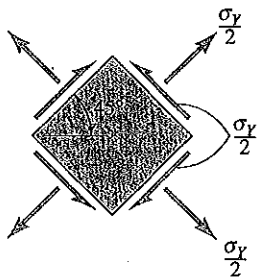
Maximum-Shear-Stress Theory:³ When a flat bar of ductile material, like mild steel, is tested in tension, it is observed that the mechanism that is actually responsible for yielding is *slip*, that is, shearing along planes of maximum shear stress at 45° to the axis of the member. Initial yielding is associated with the appearance of the first slip line on the surface of the specimen, and as the strain increases, more slip lines appear until the entire specimen has yielded. If this slip is assumed to be the actual mechanism of failure, then the stress that best characterizes this failure is the shear stress on the slip planes. Figure 12.10 shows a Mohr's circle of stress for this uniaxial stress state, indicating that the shear stress on the slip planes has a magnitude of $\sigma_Y/2$. Therefore, if it is postulated that in a ductile material under any state of stress (uniaxial, biaxial, or triaxial), failure occurs when the shear stress on any plane reaches the value $\sigma_Y/2$, then the *failure criterion* for the *maximum-shear-stress theory* may be stated as



(a) Mohr's circle for $\sigma_1 = \sigma_Y$.



(b) Principal stress element.



(c) Maximum shear-stress element.

$$\tau_{\text{abs max}} = \frac{\sigma_Y}{2} \quad (12.5)$$

where σ_Y is the yield stress determined by a simple tension test. Using Eq. 8.39 we can express Eq. 12.5 in terms of principal stresses as

$$\sigma_{\text{max}} - \sigma_{\text{min}} = \sigma_Y \quad (12.6)$$

where σ_{max} is the maximum principal stress and σ_{min} is the minimum principal stress.⁴

For the case of plane stress, the *maximum-shear-stress failure criterion* may be stated in terms of the in-plane principal stresses σ_1 and σ_2 as follows:⁵

$$\left. \begin{aligned} |\sigma_1| &= \sigma_Y \text{ if } |\sigma_1| \geq |\sigma_2| \\ |\sigma_2| &= \sigma_Y \text{ if } |\sigma_2| \geq |\sigma_1| \end{aligned} \right\} \text{ and } \sigma_1 \text{ and } \sigma_2 \text{ have same sign} \quad (12.7)$$

$$|\sigma_1 - \sigma_2| = \sigma_Y \quad \text{if } \sigma_1 \text{ and } \sigma_2 \text{ have opposite signs}$$

²The theories presented here apply only to homogeneous, isotropic materials.

³The names of C. A. Coulomb, H. Tresca, and J. J. Guest are associated with this theory of failure [Ref. 12-7].

⁴Note that this theory of failure ignores the normal stresses acting on the planes of maximum shear stress.

⁵For the case of plane stress, the out-of-plane principal stress is called σ_3 ($\sigma_3 = 0$), even though it is not necessarily the minimum principal stress.

FIGURE 12.10 Principal stresses and maximum shear stresses for a uniaxial stress test.

Equations For a me be repres If the stat the hexag to the ma

Maximum provides a re energy th theory, yi a body u specimen Cons 12.12a. T can be w

Combin

A portion and the with dist $\frac{1}{3}(\sigma_1 +$ produce



FIGURE (c) Stresse

⁶Although labeled suc ⁷This theo to M. T. H 12-7].

That is, was it due to some other failure mechanism? If the principal stress were compressive, would the failure be due to brittle fracture?

to materials fracture. Theories are expressed in terms of stress, σ_1 , σ_2 , and τ .

discussed, the

mild steel, is for yielding along the axis of the specimen on the surface. The failure of a wire specimen when the stress is high is shown in Fig. 12.10. The maximum shear stress on the surface of a ductile specimen occurs when the principal stresses are $\sigma_1 = \sigma_2 = \sigma$ and $\sigma_3 = 0$. The maximum shear stress is $\tau = \sigma/2$.

(12.5)

8.39 we can

(12.6)

principal stress, σ_1 , may be stated

(12.7)

failure [Ref. 12-7] shear stress. Although it is not

Equations 12.7 may be represented in the convenient graphical forms shown in Fig. 12.11. For a member undergoing plane stress, the state of stress at every point in the body can be represented by a *stress point* (σ_1, σ_2) in the $\sigma_1 - \sigma_2$ plane, as indicated in Fig. 12.11.⁶ The state of stress for any point in the body corresponds to a stress point that lies outside the hexagon of Fig. 12.11 or on its boundary, failure is said to have occurred according to the maximum-shear-stress theory.

Maximum-Distortion-Energy Theory:⁷ Although the maximum-shear-stress theory provides a reasonable hypothesis for yielding in ductile materials, the maximum-distortion-energy theory correlates better with test data and is therefore generally preferred. In this theory, yielding is assumed to occur when the energy associated with change of shape of a body undergoing multiaxial loading is equal to the energy of distortion in a tensile specimen when yielding occurs at the uniaxial yield stress σ_Y .

Consider the strain energy stored in an element of volume, like the one shown in Fig. 12.12a. The strain energy density due to multiaxial loading is given by Eq. 11.14, which can be written, using the three principal axes, in the form

$$u = \frac{1}{2}(\sigma_1 \epsilon_1 + \sigma_2 \epsilon_2 + \sigma_3 \epsilon_3) \quad (12.8)$$

Combining Eq. 12.8 with Hooke's Law (Eq. 2.34 with $\Delta T = 0$) we get

$$u = \frac{1}{2E}[\sigma_1^2 + \sigma_2^2 + \sigma_3^2 - 2\nu(\sigma_1 \sigma_2 + \sigma_2 \sigma_3 + \sigma_1 \sigma_3)] \quad (12.9)$$

A portion of this strain energy can be associated with the *change of volume* of the element, and the remainder of the strain energy is associated with *change of shape*, that is, with *distortion*. The change of volume is produced by the average stress $\sigma_{avg} = (\sigma_1 + \sigma_2 + \sigma_3)/3$, as illustrated in Fig. 12.12b. The net stresses shown in Fig. 12.12c

produce distortion without any change of volume.

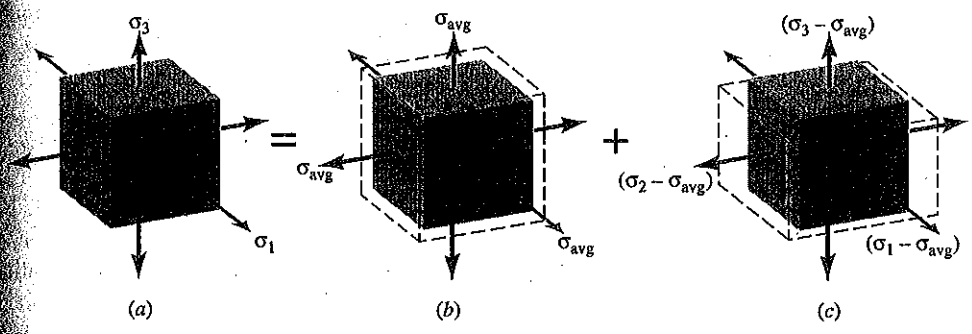
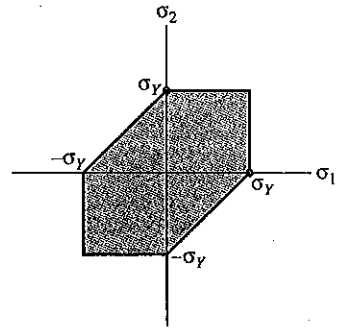


FIGURE 12.12 (a) Triaxial stress state. (b) Stresses producing volume change. (c) Stresses producing distortion.

Although σ_1 and σ_2 are principal stresses, Eq. 12.7 and Fig. 12.11 do not require that the principal axes be labeled such that $\sigma_1 \geq \sigma_2$, as was done in Chapter 8.

This theory is also called the *maximum-octahedral-shear-stress theory*. Credit for this theory is generally given to M. T. Huber, R. von Mises, and H. Hencky, although it was earlier conjectured by J. Clerk Maxwell [Ref. 12-7].



•Experimental data from tension test.

FIGURE 12.11 Failure hexagon for the maximum-shear-stress theory (plane stress).

Mechanics of Materials

R.R. Craig, Jr

626

Special Topics Related to Design

Experiments have shown that materials do not yield when they are exposed to *hydrostatic stresses*⁸ of extremely large magnitude. Therefore, it has been postulated that the stresses that actually cause yielding are the stresses that produce distortion. This hypothesis constitutes the *maximum-distortion-energy yield (failure) criterion*, which states:

Yielding of a ductile material occurs when the distortion energy per unit volume equals or exceeds the distortion energy per unit volume when the same material yields in a simple tension test.

When the distortion-producing stresses of Fig. 12.12c are substituted into Eq. 12.9 we get the following expression for the *distortion-energy density*,

$$u_d = \frac{1}{12G}[(\sigma_1 - \sigma_2)^2 + (\sigma_2 - \sigma_3)^2 + (\sigma_1 - \sigma_3)^2] \quad (12.10)$$

The distortion energy density in a tensile test specimen at the yield stress σ_Y is

$$(u_d)_Y = \frac{1}{6G}\sigma_Y^2 \quad (12.11)$$

since $\sigma_1 = \sigma_Y$ and $\sigma_2 = \sigma_3 = 0$. Therefore, yielding occurs when the distortion energy for general loading, given by Eq. 12.10, equals or exceeds the value of $(u_d)_Y$ in Eq. 12.11. Therefore, the *maximum-distortion-energy failure criterion* can be stated in terms of the three principal stresses as

$$\frac{1}{2}[(\sigma_1 - \sigma_2)^2 + (\sigma_2 - \sigma_3)^2 + (\sigma_1 - \sigma_3)^2] = \sigma_Y^2 \quad (12.12a)$$

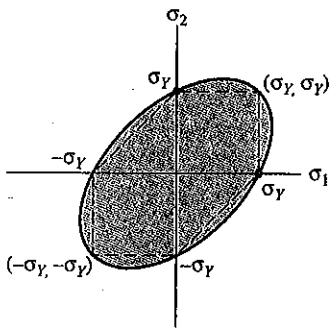
In terms of the normal stresses and shear stresses on three arbitrary mutually orthogonal planes, the maximum-distortion-energy failure criterion can be shown to have the form⁹

$$\frac{1}{2}[(\sigma_x - \sigma_y)^2 + (\sigma_y - \sigma_z)^2 + (\sigma_x - \sigma_z)^2 + 6(\tau_{xy}^2 + \tau_{yz}^2 + \tau_{xz}^2)] = \sigma_Y^2 \quad (12.12b)$$

For the case of plane stress, the corresponding expressions for the *maximum-distortion-energy yield criterion* can easily be obtained from Eqs. 12.12 by setting $\sigma_3 = \sigma_z = \tau_{xz} = \tau_{yz} = 0$. In terms of the principal stresses, then,

$$\sigma_1^2 - \sigma_1\sigma_2 + \sigma_2^2 = \sigma_Y^2 \quad (12.13)$$

This is the equation of an ellipse in the $\sigma_1 - \sigma_2$ plane, as depicted in Fig. 12.13. For comparison purposes, the failure hexagon for the maximum-shear-stress yield theory is also shown in dashed lines in Fig. 12.13. At the six vertices of the hexagon the two failure theories coincide; that is, both theories predict that yielding will occur if the state of (plane) stress at a point corresponds to any one of these six stress states. Otherwise, the maximum-shear-stress theory gives the more conservative (i.e., smaller-valued) estimate of the stresses required to produce yielding, since the hexagon falls either on or inside the ellipse.



•Experimental data from tension test.
-- Maximum-shear-stress criterion.

FIGURE 12.13 Failure ellipse for the maximum-distortion-energy theory (plane stress).

⁸Figure 12.12b represents a hydrostatic state of stress, that is, equal stresses in all three principal directions.

⁹See Sections 78 and 90 of Ref. 12-1.

A cor
root of the
that is ca
used to c

or

$$\sigma_M =$$

For the c
can easil

By c
the tensi
accordin
alent stre
form of
in the la



A forc
at the c
termin
maxim
cause f
made c

Soluti
state in
S.
quadr
point
the ra
origin

A convenient way to apply the maximum-distortion-energy theory is to take the square root of the left-hand side of Eq. 12.12a (or Eq. 12.12b) to form an equivalent stress quantity that is called the *Mises equivalent stress*. Either of the following two equations can be used to compute the Mises equivalent stress, σ_M :

$$\sigma_M = \frac{\sqrt{2}}{2} [(\sigma_1 - \sigma_2)^2 + (\sigma_2 - \sigma_3)^2 + (\sigma_1 - \sigma_3)^2]^{1/2} \quad (12.14a)$$

or

$$\sigma_M = \frac{\sqrt{2}}{2} [(\sigma_1 - \sigma_2)^2 + (\sigma_2 - \sigma_3)^2 + (\sigma_1 - \sigma_3)^2 + 6(\tau_{xy}^2 + \tau_{yz}^2 + \tau_{xz}^2)]^{1/2} \quad (12.14b)$$

For the case of plane stress, the corresponding expressions for the Mises equivalent stress can easily be obtained from Eqs. 12.14 by setting $\sigma_3 = \sigma_z = \tau_{xz} = \tau_{yz} = 0$.

By comparing the value of the Mises equivalent stress at any point with the value of the tensile yield stress, σ_y , it can be determined whether yielding is predicted to occur according to the maximum-distortion-energy theory of failure. Therefore, the Mises equivalent stress is widely used when calculated stresses are presented in tabular form or in the form of color stress plots, as has been done for the finite element analysis results shown in the last picture in the color-photo insert.

EXAMPLE 12.3

A force P_0 kips applied by a lever arm to the shaft in Fig. 1 produces stresses at the critical point A having the values shown on the element in Fig. 1. Determine the load $P_S \equiv c_S P_0$ that would cause the shaft to fail according to the maximum-shear-stress theory, and determine the load $P_D \equiv c_D P_0$ that would cause failure according to the maximum-distortion-energy theory. The shaft is made of steel with $\sigma_Y = 36$ ksi.

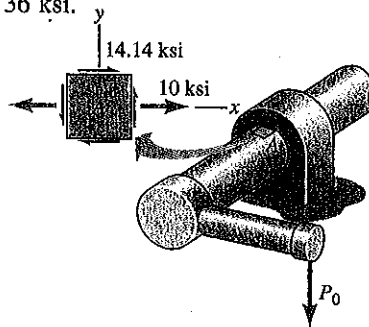


Fig. 1

Solution It will be helpful if we construct a Mohr's circle for the plane stress state in Fig. 1 and also sketch the failure envelopes for the two failure theories.

Since σ_1 is positive and σ_2 is negative, we only need to sketch the fourth quadrant of the failure envelope. This is shown in Fig. 3. Since the stresses at point A are proportional to load, the stresses due to any load cP_0 will lie along the radial line identified in Fig. 3 as the *load line*. This line passes through the origin of the $\sigma_1 - \sigma_2$ plane and through the stress point ($\sigma_{1P} = 20$ ksi,

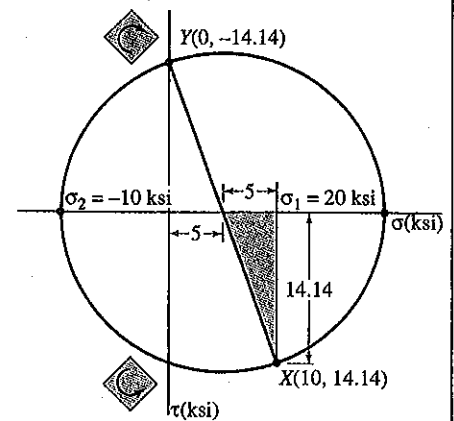


Fig. 2 Mohr's circle for stress state at point A.

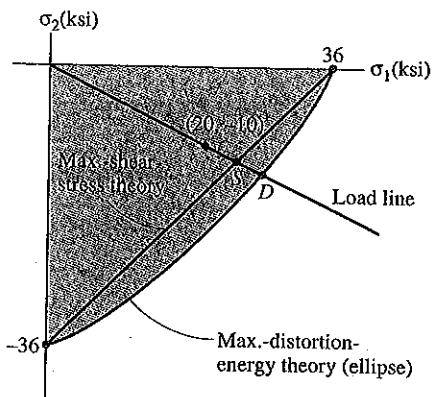


Fig. 3 Fourth quadrant of failure envelopes.

$\sigma_{2P} = -10$ ksi) that corresponds to the principal stresses due to load P_0 . Failure according to the maximum-shear-stress theory occurs at the stress state marked S in Fig. 3, and failure according to the maximum-distortion-energy theory occurs at point D .

Maximum-Shear-Stress Theory. Point S is the intersection of the load line given by

$$\sigma_1 = -2\sigma_2 \quad (1)$$

and the maximum-shear-stress boundary line

$$\sigma_1 - \sigma_2 = \sigma_Y = 36 \text{ ksi} \quad (2)$$

Solving Eqs. (1) and (2) for σ_1 and σ_2 we get

$$\sigma_{1S} = 24 \text{ ksi}, \quad \sigma_{2S} = -12 \text{ ksi}$$

Combining these values with σ_1 and σ_2 of Fig. 2 we get

$$c_S = \frac{P_S}{P_0} = \frac{\sigma_{1S}}{\sigma_{1P}} = \frac{24 \text{ ksi}}{20 \text{ ksi}} = 1.2$$

$$c_S = 1.2$$

Ans.

Maximum-Distortion-Energy Theory: Point D in Fig. 3 is the intersection of the load line, given by Eq. (1), and the parabola given by Eq. 12.13. Thus,

$$\sigma_{1D}^2 - \sigma_{1D}\sigma_{2D} + \sigma_{2D}^2 = \sigma_Y^2 = (36 \text{ ksi})^2 \quad (3)$$

Combining Eqs. (1) and (3) gives

$$7\sigma_{2D}^2 = (36 \text{ ksi})^2$$

Then, since $\sigma_1 > 0$ and $\sigma_2 < 0$, we get

$$\sigma_{1D} = 27.21 \text{ ksi}, \quad \sigma_{2D} = -13.61 \text{ ksi}$$

Comparing these stresses with the principal stresses produced by P_0 gives

$$c_D = \frac{P_D}{P_0} = \frac{\sigma_{1D}}{\sigma_{1P}} = \frac{27.21 \text{ ksi}}{20 \text{ ksi}} = 1.36$$

$$c_D = 1.36$$

Ans.

We could get this same result by noting that the factor of safety against yielding, according to the maximum-distortion-energy yield criterion is given by

$$FS_d = \sigma_Y / \sigma_M$$

where σ_M

$$\sigma_M = \sigma$$

Then,

In su
the maxim
cause fail
der load
to failure
of $FS_d =$
energy th

Brittle M
imum-norr

Maximum
2.15b, that
yielding. A
test, a bar
stress. Exp
this biaxia
uniaxial te
an object
material re
test. This t
value as d

For th
the equatio

These equ

Mohr's Fa
not equal t
be used. A
failure cri
uniaxial co
an ultimat

¹⁰Also called
Glasgow Un

¹¹As in Figs.

¹²This theory

where σ_M is the Mises equivalent stress. For the original load P_0 ,

$$\sigma_M = \sigma_1^2 - \sigma_1\sigma_2 + \sigma_2^2 = [(20)^2 - (20)(-10) + (-10)^2] = 26.46 \text{ ksi}$$

Then,

$$FS_d = \frac{\sigma_Y}{\sigma_M} = \frac{36 \text{ ksi}}{26.46 \text{ ksi}} = 1.36$$

In summary, a 20% increase in the load would cause failure according to the maximum-shear-stress theory, but a 36% increase would be required to cause failure according to the maximum-distortion-energy theory. That is, under load P_0 the member would have a factor of safety $FS_s = 1.2$ with respect to failure according to the maximum-shear-stress theory and a factor of safety of $FS_d = 1.36$ with respect to failure according to the maximum-distortion-energy theory of failure.

Brittle Materials. Two theories of failure for brittle materials are presented, the maximum-normal-stress theory and Mohr's failure theory.

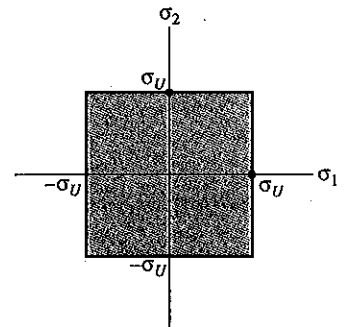
Maximum-Normal-Stress Theory:¹⁰ It was stated in Section 2.4 and illustrated in Fig. 2.15b, that in a tension test, a brittle material fails suddenly by *fracture*, without prior yielding. And it was stated in Section 4.5 and illustrated in Fig. 4.19b, that in a torsion test, a bar made of brittle material also fails by fracture on planes of maximum tensile stress. Experiments have shown that the value of the normal stress on the failure plane for this biaxial state of stress is not significantly different from the fracture stress σ_U in a uniaxial tensile test. Therefore, the hypothesis of the *maximum-normal-stress theory* is that an object made of brittle material will fail when the maximum principal stress in the material reaches the ultimate normal stress that the material can sustain in a uniaxial tension test. This theory also assumes that compression failures occur at the same ultimate stress value as do tension failures.

For the case of *plane stress*, the *maximum-normal-stress failure criterion* is given by the equations

$$\sigma_1 = \sigma_U \quad \text{or} \quad \sigma_2 = -\sigma_U \quad (12.15)$$

These equations may be plotted on the $\sigma_1 - \sigma_2$ plane, as shown in Fig. 12.14.¹¹

Mohr's Failure Criterion:¹² If the ultimate compressive strength of a brittle material is not equal to its ultimate strength in tension, the maximum-normal-stress theory should not be used. An alternative failure theory was proposed by Otto Mohr and is called *Mohr's failure criterion*. Figure 12.15a shows Mohr's circles for a uniaxial tensile test and for a uniaxial compression test for a brittle material having a tensile ultimate strength σ_{TU} and an ultimate strength in compression of σ_{CU} . By Mohr's theory, when σ_1 and σ_2 have the



•Experimental data from tension test.

FIGURE 12.14 Failure diagram for the maximum-normal-stress theory (plane stress).

¹⁰Also called *Rankine's Theory* after W. J. M. Rankine (1820–1872), an eminent professor of engineering at Glasgow University in Scotland.

¹¹As in Figs. 12.11 and 12.13, σ_1 is not necessarily the greater principal stress.

¹²This theory is named for the German engineer Otto Mohr (1835–1918), the developer of Mohr's circle.

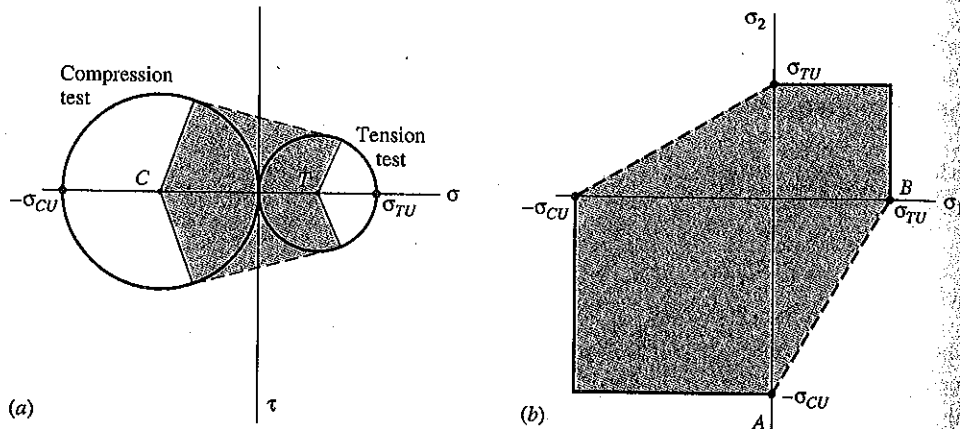


FIGURE 12.15 Mohr's failure criterion (plane stress).

same sign, failure occurs if either of the following stress limits is reached:

$$\sigma_{\max} = \sigma_{TU} \quad \text{or} \quad \sigma_{\min} = -\sigma_{CU} \quad (12.16)$$

These equations are plotted as solid-line boundaries in Fig. 12.15b. For cases where σ_1 and σ_2 have opposite signs, Mohr proposed that the failure boundary be determined by drawing tangents to the tension and compression circles, as illustrated by the dashed lines in Fig. 12.15a. It can be shown (see Example 12.4) that the principal stresses for all circles that have centers on the σ -axis and are tangent to the dashed tangent lines in Fig. 12.15a plot as points on the dashed-line boundaries in Fig. 12.15b. If torsion test data or other plane-stress failure data are available, the failure boundaries in the second and fourth quadrants of Fig. 12.6b can be modified to incorporate these experimental data (e.g., see *Modified Mohr Theory* in Ref. [12-8]).

EXAMPLE 12.4

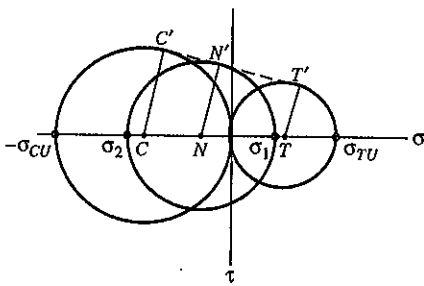


Fig. 1

Show that, for $\sigma_1 > 0$ and $\sigma_2 < 0$, the stress points that lie on the dashed line AB in Fig. 12.15b correspond to the principal stresses on Mohr's circles that have centers lying between points C and T in Fig. 12.15a and are tangent to the dashed lines in this figure.

Solution Let us redraw Fig. 12.15a and add an intermediate circle as specified in the problem statement (Fig. 1). The equation of the dashed-line AB in Fig. 12.15b is

$$\sigma_2 = \sigma_{CU} \left(\frac{\sigma_1}{\sigma_{TU}} - 1 \right) \quad (1)$$

We are to prove that this equation is the equation that relates the principal stresses σ_1 and σ_2 for the circle with center at N in Fig. 1. From Fig. 1,

$$\sigma_1 = \sigma_n + \overline{NN'}, \quad \sigma_2 = \sigma_n - \overline{NN'} \quad (2)$$

where σ_n is the normal stress corresponding to point N . Also, from Fig. 1, the centers of the tension-test Mohr's circle and the compression-test Mohr's circle

are

and their

Let

That is,

Then, the equation

or

Con

The eliminated dashed

*12.4

At some paper-clip did not o large plas in the wir cycles of many me any case, fracture u

¹³Fatigue fa was used b railway eng

are

$$\sigma_t = \frac{\sigma_{TU}}{2}, \quad \sigma_c = -\frac{\sigma_{CU}}{2} \quad (3)$$

and their radii are

$$\overline{TT'} = \frac{\sigma_{TU}}{2}, \quad \overline{CC'} = \frac{\sigma_{CU}}{2} \quad (4)$$

Let

$$\sigma_n = \sigma_c + k(\sigma_t - \sigma_c)$$

That is,

$$\sigma_n = -\frac{\sigma_{CU}}{2} + k\left(\frac{\sigma_{TU}}{2} + \frac{\sigma_{CU}}{2}\right) \quad (5)$$

Then, the radius $\overline{NN'}$ will be linearly related to the radii $\overline{CC'}$ and $\overline{TT'}$ by the equation

$$\overline{NN'} = \overline{CC'} - k(\overline{CC'} - \overline{TT'})$$

or

$$\overline{NN'} = \frac{\sigma_{CU}}{2} - k\left(\frac{\sigma_{CU}}{2} - \frac{\sigma_{TU}}{2}\right) \quad (6)$$

Combining Eqs. (2), (5), and (6), we get

$$\sigma_1 = k\sigma_{TU}, \quad \sigma_2 = \sigma_{CU}(k - 1) \quad (7)$$

The elimination of k from Eqs. (7) produces Eq. 1, the desired equation of the dashed line AB in Fig. 12.15b. QED.

12.4 FATIGUE AND FRACTURE

At some time or other you have probably held a paper clip in your hands and bent the paper-clip wire back and forth several times until the wire finally broke in two. The failure did not occur when the paper clip was first bent, even though the wire experienced very large plastic deformation. Instead, failure occurred after a few reversals of flexural stress in the wire. This type of failure is called *fatigue failure*.¹³ If the failure occurs after a few cycles of loading, perhaps up to a thousand cycles, it is called *low-cycle fatigue*. However, many metal components experience fatigue failure only after millions of stress cycles. In any case, when failure occurs at a stress level that is less than the level that would produce fracture under a single static application of load, the failure is called a fatigue failure.

¹³Fatigue failure of axles of railway cars was a source of great concern and study in the 1800s. The term *fatigue* was used by Poncelet to denote this type of failure due to cyclic stresses. A. Wöler (1819–1914), a German railway engineer, is credited with developing the first fatigue testing machine. [Ref. 12-7]

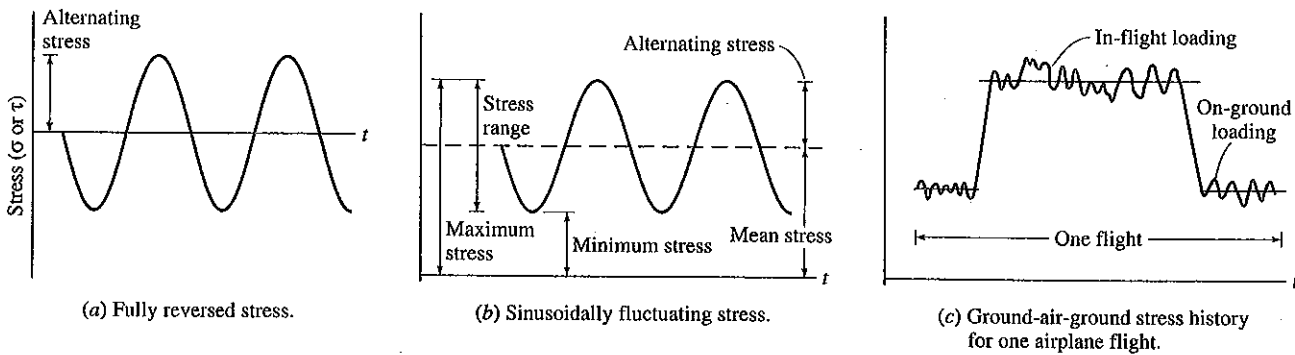


FIGURE 12.16 Typical cyclic stresses that can produce fatigue failure.

The types of fluctuating stresses that lead to fatigue failure in metals are illustrated in Fig. 12.16. Figure 12.16a is the type of fully reversed stress that would be experienced by a railway-car axle as the train moves at constant speed along the track. Figure 12.16b shows a superposition of a (constant) mean stress and a sinusoidally varying stress; Fig. 12.16c illustrates the more complicated type of fluctuating stress experienced, for example, by an airplane wing component during a single flight. The fracture that occurs as a result of such fluctuating stresses usually begins at a point of stress concentration (Section 12.2) like the edge of the fastener hole in the splice plate shown in Fig. 12.17a and the airplane wing leading-edge nose cap in Fig. 12.17b. The crack is initiated in a region of high stress intensity, usually at some microscopic flaw or imperfection. Stress cycles cause the fatigue crack to grow slowly in size until the crack reaches a *critical crack length*, at which point the crack propagates at an explosive rate leaving the component unable to sustain load. Figure 12.17c shows the typical “beach-sand markings” of a fatigue fracture surface. Along the bottom edge of this photo, two points of initiation of the fatigue crack can be identified; the “ridges” on the fracture surface indicate the progress of the crack as it propagated with successive cycles of stress.

To characterize the behavior of a material under repeated cycles of loading, *fatigue tests* at various levels of stress are performed, and the results are plotted as an *S-N diagram*,

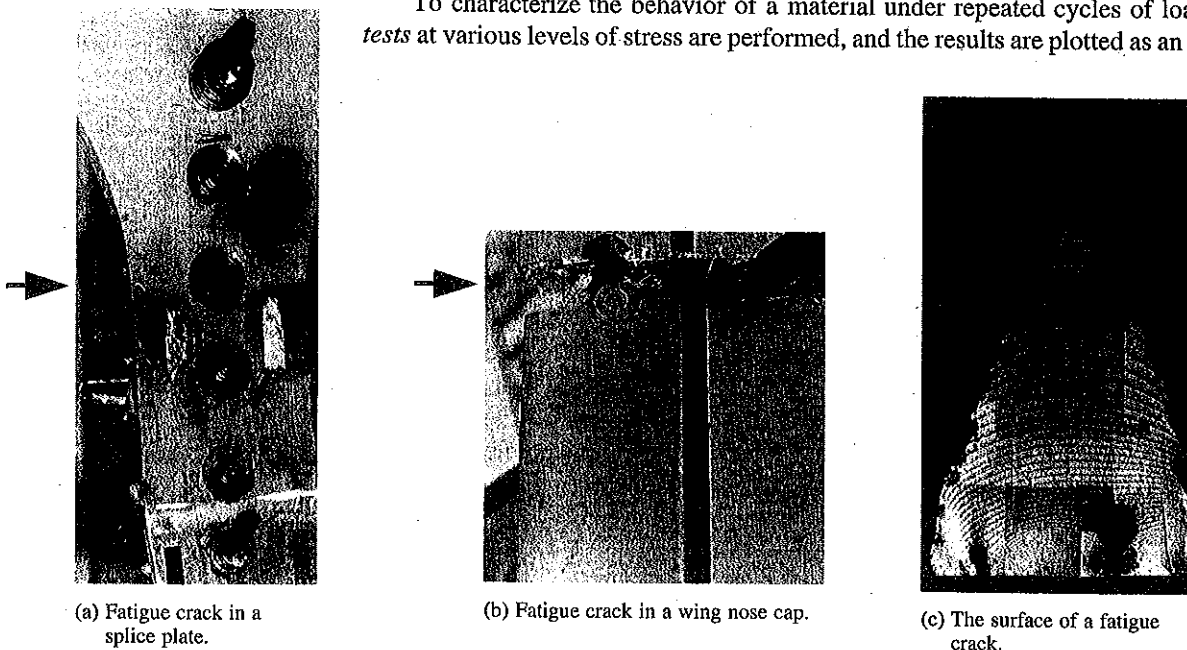


FIGURE 12.17 Examples of fatigue cracks. (Used with permission, Lockheed Fort Worth Company, 1993.)

Nominal stress (MPa)

or *endurance* tests. Initially identified by ten tests at various maximum amplitudes of cycles. Similar tests are plotted as *S-N* diagrams. The *e* there is a which a *v* fatigue fa alloys, ba of the ste

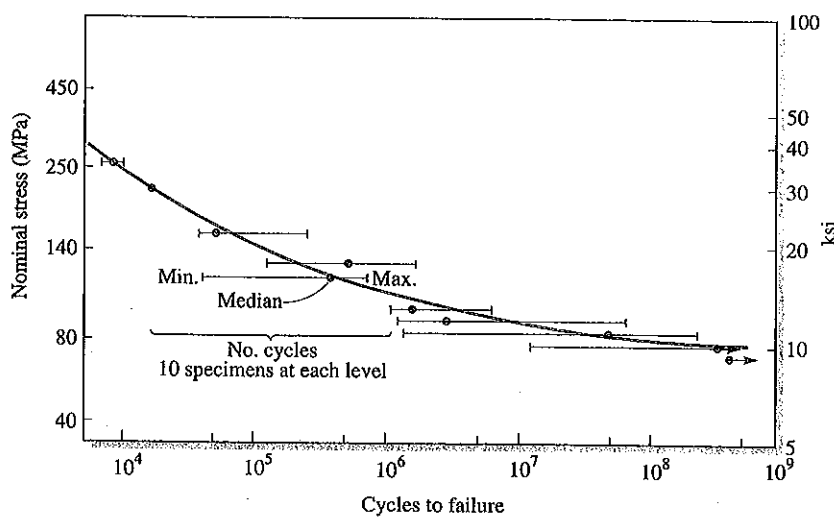
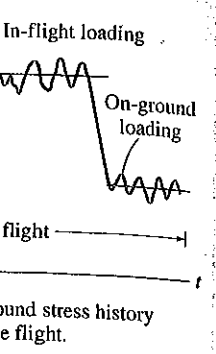


FIGURE 12.18 An S-N diagram for 7075-T6 aluminum alloy notched tensile specimens. (From Ref. 12-10.)

... are illustrated in ...
 ... be experienced by ...
 ... Figure 12.16b ...
 ... varying stress; Fig. ...
 ... experienced, for example, ...
 ... at occurs as a result ...
 ... (Section 12.2) ...
 ... 17a and the airplane ...
 ... region of high stress ...
 ... cause the fatigue ...
 ... length, at which point ...
 ... able to sustain load. ...
 ... ue fracture surface. ...
 ... atigue crack can be ...
 ... s of the crack as it

... or *endurance curve*.¹⁴ Figure 12.18 is an S-N diagram based on a series of tests on nominally identical test specimens. (Note that the diagram is a log-log plot.) Several tests (e.g., ten tests at each stress level for Fig. 12.18) are conducted with cyclic stress whose maximum amplitude is slightly less than the ultimate static strength of the material. The number of cycles of stress required to cause fracture at that stress level is recorded for each test. Similar test series are conducted at progressively lower levels of stress, and the results plotted as the number of cycles to cause fatigue failure in each test. The scatter band for the tests at various stress levels are indicated on Fig. 12.18.

The endurance curves for some materials have the form illustrated in Fig. 12.19, where there is a stress level, called the *fatigue level*, or *endurance limit*, of the material, below which a virtually infinite number of stress cycles can be sustained without resulting in a fatigue failure. Many steel alloys exhibit this type of behavior. Fatigue limits for steel alloys, based on 10^7 stress cycles, are typically 35%–60% of the ultimate tensile strength of the steel.¹⁵ As indicated in Fig. 12.19, notches or other imperfections obviously degrade

... of loading, *fatigue* ...
 ... as an *S-N diagram*,

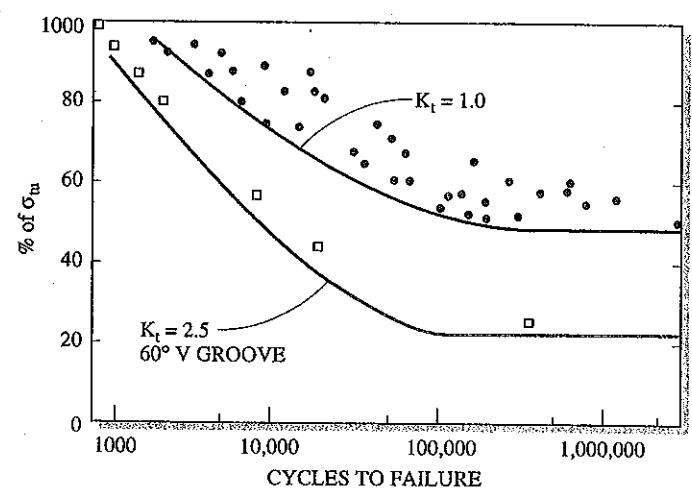


FIGURE 12.19 An S-N diagram for steel round-bar rotating-beam specimens. (Ref. 12-11, maintained and published by CINDAS/Purdue University under Cooperative Research and Development Agreement with the U.S. Air Force. Used with permission.)



... gue ...
 ... kheed Fort Worth

¹⁴Test procedures to produce S-N diagrams are described in ASTM Standards E466-E468. [Ref. 12-9]
¹⁵*Structural Alloys Handbook*. [Ref. 12-11]